

Acridinium-Based Photocatalysts: A Sustainable Option in Photoredox Catalysis

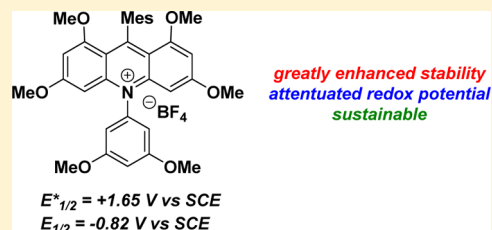
Amruta Joshi-Pangu,[†] François Lévesque,[†] Hudson G. Roth,[‡] Steven F. Oliver,[†] Louis-Charles Campeau,[†] David Nicewicz,[‡] and Daniel A. DiRocco^{*,†}

[†]Process Research & Development, Merck Research Laboratories, P.O. Box 2000, Rahway, New Jersey 07065, United States

[‡]Department of Chemistry, University of North Carolina at Chapel Hill, Chapel Hill, North Carolina 27599-3290, United States

Supporting Information

ABSTRACT: The emergence of visible light photoredox catalysis has enabled the productive use of lower energy radiation, leading to highly selective reaction platforms. Polypyridyl complexes of iridium and ruthenium have served as popular photocatalysts in recent years due to their long excited state lifetimes and useful redox windows, leading to the development of diverse photoredox-catalyzed transformations. The low abundances of Ir and Ru in the earth's crust and, hence, cost make these catalysts unsustainable and have limited their application in industrial-scale manufacturing. Herein, we report a series of novel acridinium salts as alternatives to iridium photoredox catalysts and show their comparability to the ubiquitous $[\text{Ir}(\text{dF-CF}_3\text{-ppy})_2(\text{dtbpy})](\text{PF}_6)$.



INTRODUCTION

In the past decade, visible light photoredox catalysis has revolutionized the manner in which chemists approach new bond formations. Polypyridyl complexes of ruthenium and iridium are among the most widely utilized photocatalysts due to their unique photophysical properties such as long excited state lifetimes and large redox windows (Figure 1).¹ For

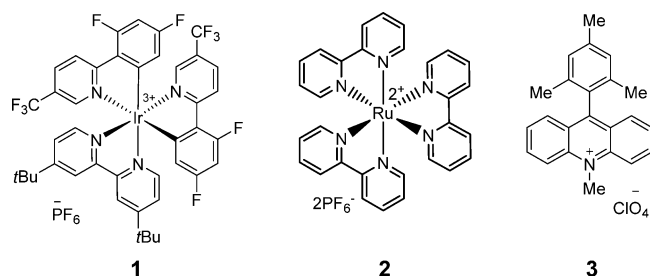


Figure 1. Commonly used photocatalysts $\text{Ir}(\text{dF-CF}_3\text{-ppy})_2(\text{dtbbpy})(\text{PF}_6)_3$, $\text{Ru}(\text{bpy})_3(2\text{PF}_6)_2$, and 9-mesityl-10-methylacridinium perchlorate.

example, the photophysical properties of ruthenium tris-(bipyridine) (**2**) have been thoroughly studied. $\text{Ru}(\text{bpy})_3^{2+}$ has a long-lived excited state lifetime (1100 ns) and excited state redox potentials of $E_{1/2}(\text{III}^*/\text{II}) = -0.81 \text{ V}$ and $E_{1/2}(*\text{II}/\text{I}) = +0.77 \text{ V}$ vs SCE (Table 1) that allow it to engage in a variety of oxidative and reductive processes.²

$[\text{Ir}(\text{dF-CF}_3\text{-ppy})_2(\text{dtbpy})](\text{PF}_6)$ (**1**), initially reported for OLED and water-splitting applications,³ has likewise become one of the most widely used photocatalysts in recent years. While it bears many similarities to $\text{Ru}(\text{bpy})_3^+$, it offers a longer-lived excited state lifetime (2300 ns) and greatly expanded

redox window ($E_{1/2}(\text{Ir}(\text{III}^*/\text{II})) = 1.21 \text{ V}$ and $E_{1/2}(\text{Ir}(\text{III}^*/\text{IV})) = -0.89 \text{ V}$). Owing to the low abundance of iridium in earth's crust (0.001 ppm),⁴ Ir-based photocatalysts are viewed as neither cost-effective nor sustainable. From an industrial perspective, organic-based photocatalysts represent a cost-effective and sustainable approach to photoredox catalysis. Inspired by the unique reactivity of $[\text{Ir}(\text{dF-CF}_3\text{-ppy})_2(\text{dtbpy})](\text{PF}_6)$ (**1**), we were interested in developing an organic photoredox catalyst scaffold that is robust, has a useful redox window, and is easily synthesized on a commercial scale. Highly reducing organic photoredox catalysts, such as 10-phenylphenothiazine (PTH; $E_{1/2}^* = -2.1 \text{ V}$ vs SCE) have shown utility in replacing transition-metal complexes such as $\text{Ir}(\text{ppy})_3$ ($E_{1/2}^* = -1.7 \text{ V}$ vs SCE) in reductively initiated reactions, due to their similar excited state reduction potentials.⁵ No similar scaffold has been demonstrated to replace $[\text{Ir}(\text{dF-CF}_3\text{-ppy})_2(\text{dtbpy})](\text{PF}_6)$ in reactions initiated via oxidation.⁶

Initially, we considered using the traditional xanthene-based scaffold upon which fluorescein, rose bengal, and eosin Y are based.⁷ However, their narrow redox window, low solubility in typical organic solvents, pH dependence, and susceptibility to bleaching have rendered this class of catalysts less effective. Acridinium-based photocatalysts appear to obviate many of these pitfalls, as they have extended redox windows in comparison to other organo-photocatalysts, are insensitive to the pH of the reaction medium, and are soluble in a range of organic solvents. 9-Mesityl-10-methylacridinium perchlorate (**3**), pioneered by Fukuzumi,⁸ has been utilized effectively in

Special Issue: Photocatalysis

Received: May 24, 2016

Published: July 25, 2016

Table 1. Photophysical Properties of Photocatalysts 1–8

entry	photocatalyst	$E_{1/2}(C^+/C^*)$ (V)	$E_{1/2}(C^*/C^-)^a$ (V)	$E_{1/2}(C^+/C)$ (V)	$E_{1/2}(C/C^-)^b$ (V)	excited state lifetime τ (ns)	excitation λ_{max} (nm)	emission λ_{max} (nm)
1	[Ir(dF-CF ₃ -ppy) ₂ (dtbpy)] (PF ₆) (1)	-0.89	+1.21	+1.69	-1.37	2300	380	470
2	[Ru(bpy) ₃](PF ₆) ₂ (2)	-0.81	+0.77	+1.29	-1.33	1100	452	615
3	acridinium (3)		+2.06		-0.57	$t_F = 6.4$ ns	430	570
4	acridinium (4)		+2.08		-0.59	$t_F = 14.4$ ns	420	517
5	acridinium (5)		+1.90		-0.57	$t_F = 18.7$ ns	466	545
6	acridinium (6)		+2.01		-0.71	$t_{F1} = 3.0$ ns, $t_{F2} = 10.1$ ns	407	525
7	acridinium (7)		+1.65		-0.82	$t_{F1} = 1.3$ ns, $t_{F2} = 12.3$ ns	414	550
8	acridinium (8)		+1.62		-0.84	$t_{F1} = 1.3$ ns, $t_{F2} = 8.9$ ns	412	550

^aExcited state reduction potentials were estimated from ground state redox potentials and the intersection of the absorption and emission bands.

^bDetermined by cyclic voltammetry in acetonitrile versus SCE. See the Supporting Information.

a variety of transformations, most notably in the anti-Markonikov addition of nucleophiles to olefins.⁹ While uniquely applicable to chemistries that require strong single electron oxidants, it is limited in many transformations due to its weakly negative ground state reduction potential ($E_{1/2}(C/C^-) = -0.57$ V vs SCE). Furthermore, its strongly positive excited state reduction potential ($E^*_{1/2} = +2.06$ V vs SCE) can lead to substrate decomposition through unselective oxidation processes. Studies have shown that catalyst 3 undergoes demethylation and is prone to nucleophilic attack, leading to degradation and bleaching of the catalyst chromophore.¹⁰ We hoped to overcome these shortcomings by designing acridinium catalysts with enhanced stability and attenuated excited state reduction potentials. Herein, we describe a modular series of readily accessible novel acridinium photocatalysts with increased physical stability and expanded redox windows.

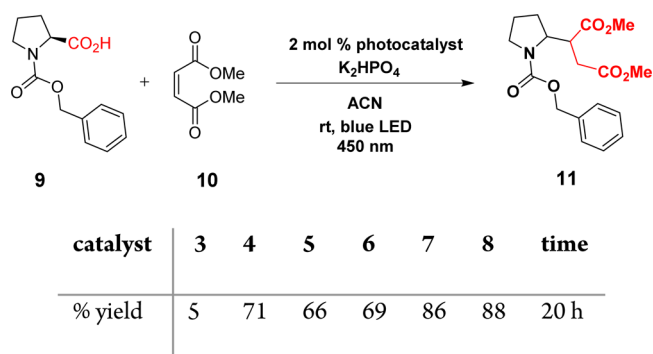
RESULTS AND DISCUSSION

A series of substituted acridinium salts were synthesized to probe the relationship between structure and the physical properties of these novel catalysts. The acridinium nitrogen was arylated to avoid the competitive demethylation previously observed with the corresponding *N*-methyl catalyst. The presence of electron-donating substituents on the acridinium core results in longer excited state lifetimes (8.9–18.7 ns) and, in the case of catalysts 6–8, a more negative ground state reduction potential in comparison to the parent catalyst 3 (Table 1). In particular, tetramethoxy-substituted acridinium 8 was measured to possess a ground state redox potential ($E_{1/2}(C/C^-) = -0.84$ V vs SCE) comparable to the excited state redox potential of [Ir(dF-CF₃-ppy)₂(dtbpy)](PF₆) ($E_{1/2}(C^+/C^*) = -0.89$ V vs SCE).

With these promising results in hand, we next investigated the reactivity of these catalysts in the decarboxylative conjugate addition of Cbz-proline (9) to dimethyl maleate (10), which is known to be catalyzed by [Ir(dF-CF₃-ppy)₂(dtbpy)](PF₆)

(Scheme 1).¹¹ In the presence of the Fukuzumi catalyst 3, very low conversion to product was observed. Given the measured

Scheme 1. Decarboxylative Conjugate Addition of Cbz-Proline to Dimethyl Maleate



photophysical properties of the new acridinium catalysts, base-promoted deprotonation of Cbz-proline and single electron transfer of the carboxylate (hexanoate, $E_{1/2}(\text{red}) = +1.16$ V vs SCE) and single electron reduction of the resultant α -acyl radical (α -acyl radical, $E_{1/2}(\text{red}) = -0.60$ V vs SCE) upon Michael addition should be thermodynamically favorable (Figure 2).¹¹ Gratifyingly, high yields were obtained when Cbz-proline was reacted with dimethyl maleate in acetonitrile using the substituted acridinium salts 4–8 (Scheme 1). Catalysts 7 and 8 performed exceptionally well, consistent with their more negative ground state reduction potentials (Table 1, entries 7 and 8).

We chose catalyst 7 for further studies due to its high catalytic activity and straightforward synthesis (Scheme 2, Figure 3, and Tables 2 and 3).¹² To determine the feasibility of using this catalyst on a larger scale and avoid problems associated with scale in batch photochemistry, we further studied the reaction using a flow reactor.¹³ In an attempt to improve

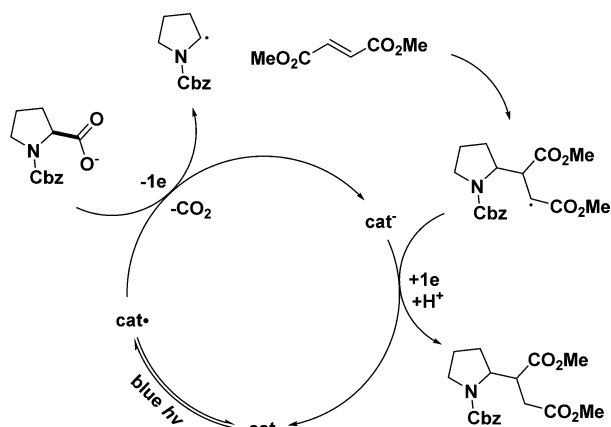


Figure 2. Proposed mechanism of the photocatalyzed decarboxylative conjugate addition of Cbz-proline to dimethyl maleate.

productivity, higher reaction concentrations were examined but proved detrimental to the reaction rate. Catalyst loading had little to no effect (Table 2), characteristic of a light-limited process. The reaction rate and yield increased with increasing reaction temperature, albeit with significant concomitant catalyst degradation.¹⁴ Furthermore, the observed rate of Cbz-proline consumption was significantly faster than that of dimethyl maleate (Figure 3). Ultimately, increasing the amount of dimethyl maleate from 1.0 to 1.5 equiv while running the reaction at 40 °C resulted in optimal conditions for the flow process (Table 3). We obtained an 89% yield (HPLC assay) of the desired product with a 60 min residence time (Figure 3).

To gain a further understanding of the large difference in reactivity between the Fukuzumi catalyst 3 and catalyst 7, we monitored their respective concentrations at different residence times. While catalyst 7 did show some decomposition over the course of the reaction, Fukuzumi catalyst 3 was completely degraded within 2 min (Figure 4). This observation further underscores the effectiveness of the alterations to the parent mesitylacridinium scaffold to enhance the stability of this important class of photoredox catalysts.

In conclusion, we have developed a series of 1,3,5,6-substituted acridinium salts as organic alternatives to transition-metal-based photocatalysts that combine a useful redox window and higher chemical stability. The tetrasubstituted catalysts can be obtained in a single step from the corresponding triarylamine and have shown catalytic performance comparable to that of $[\text{Ir}(\text{dF-CF}_3\text{-ppy})_2(\text{dtbpy})](\text{PF}_6)$ in the decarboxylative conjugate addition of Cbz-proline to dimethyl maleate. Given the sustainable, cost-effective, and robust nature of these novel catalysts, we plan to continue

Scheme 2. Synthesis of Acridinium Salt Photocatalyst 7

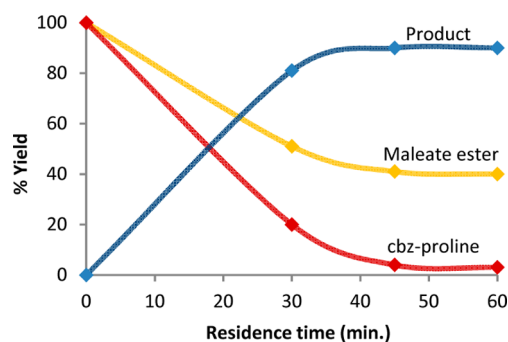
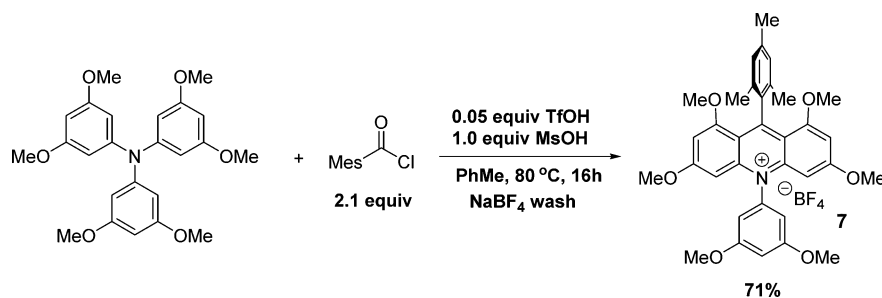


Figure 3. Reaction progress analysis: Cbz-proline (1 mmol), dimethyl maleate (1.5 mmol), catalyst 7 (0.012 mmol), 2,6-lutidine (1.2 mmol), biphenyl (0.1 mmol), acetonitrile (10 mL). The reaction yield was calculated via HPLC using biphenyl as internal standard.

Table 2. Initial Reaction Optimization in Flow^a

entry	(M)	amt of cat. (mol %)	temp (°C)	yield (%) ^b
1	0.08	1	30	43
2	0.16	1	30	30
3	0.4	1	30	18
4	0.16	0.5	30	33
5	0.16	1	30	30
6	0.16	2	30	29
7	0.08	1	40	63
8	0.08	1	60	80

^aStandard reaction conditions: Cbz-proline (1 mmol), dimethyl maleate (1 mmol), 2,6-lutidine (1.2 mmol), biphenyl (0.1 mmol), in acetonitrile, 30 min residence time. Flow experiments were carried out using a Vaportec R2S equipped with a UV-150 photoreactor (10 mL, FEP tubing, 1.3 mm i.d.). ^bReaction yield calculated via HPLC using biphenyl as internal standard.

Table 3. Reaction Optimization Results in Flow ($\tau = 60$ min)^a

entry	amt of 9 (equiv)	amt of 10 (equiv)	temp (°C)	yield (%) ^b
1	1.0	1.0	60	80
2	1.2	1.0	40	82
3	1.0	1.5	40	89

^aFlow experiments were carried out using a Vaportec R2S equipped with a UV-150 photoreactor (10 mL, FEP tubing, 1.3 mm i.d.). ^bReaction yield calculated via HPLC using biphenyl as internal standard.

evaluating their performance in photochemical reactions with an eye toward their future implementation in manufacturing processes.

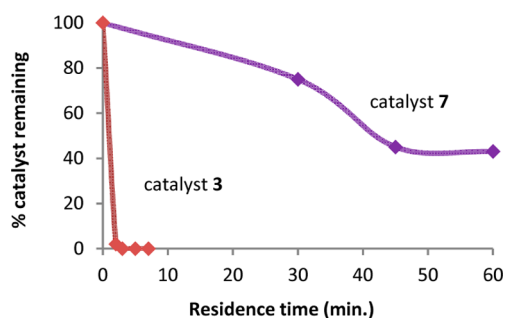


Figure 4. Catalyst degradation analysis for catalysts 3 and 7: Cbz-proline (1 mmol), dimethyl maleate (1.5 mmol), catalyst (0.012 mmol), 2,6-lutidine (1.2 mmol), biphenyl (0.1 mmol), acetonitrile (10 mL). The reaction yield was calculated via HPLC using biphenyl as internal standard.

EXPERIMENTAL SECTION

General Methods. All reactions were carried out under nitrogen outside the glovebox. 3,6-Di-*tert*-butyl-9-mesityl-10-phenylacridin-10-ium was synthesized via a reported method.¹¹ 9-Mesityl-10-methylacridinium perchlorate was purchased from TCL. ¹H NMR spectra were recorded on either a 500 or 600 MHz spectrometer at ambient temperature. Data are reported as follows: chemical shift in parts per million (δ , ppm) from residual CHCl₃ (7.26 ppm), multiplicity (*s* = singlet, *bs* = broad singlet, *d* = doublet, *t* = triplet, *q* = quartet, *m* = multiplet, *om* = overlapped multiplet, and *dd* = doublet of doublets), coupling constants (Hz), and number of protons (H). ¹³C NMR spectra were recorded on either a 500 or 600 MHz spectrometer at ambient temperature. Chemical shifts are reported in ppm from CDCl₃ (77.16 ppm). Reactions were monitored using UPLC-MS. Crude reactions were purified using flash column chromatography.

General Procedure for Reactions in Scheme 1. In a 1 dram vial equipped with a stir bar were placed (*S*)-1-((benzyloxy)carbonyl)-pyrrolidine-2-carboxylic acid (20 mg, 0.08 mmol), dimethyl maleate (11 μ L, 0.088 mmol), catalyst (2 mol %, 1.605 μ mol), and K₂HPO₄ (16.77 mg, 0.096 mmol) in acetonitrile (2 mL). The reaction was degassed by bubbling nitrogen through the reaction mixture for 15 min. Seven reactions for catalysts 2–8 and catalyst 1 were set up in parallel inside a Dewar flask. The 450 nm blue LED lamp was placed over the Dewar, and the setup was covered with aluminum foil. The reaction temperature was maintained between 30 and 35 °C by adjusting the flow of nitrogen through the Dewar. Reaction mixtures were irradiated for 20 h and assayed via HPLC against internal standard to calculate the assay yield.

General Setup for Reactions in Flow. A Vaportec R2S (peristaltic pump, blue tube) and R4 modules equipped with a UV-150 photoreactor (10 mL, FEP tubing, 1.3 mm i.d.) were used. The photoreactor was fitted with a 450 nm LED lamp (input power 60 W, radiant power 24 W). The photoreactor was either cooled (Vaportec cooling module) or heated. The exiting stream was connected to a UV detector (Knauer, Detector 50D) to trigger collection. A variable back-pressure regulator was attached, and the internal pressure was maintained around 2.1 bar. Finally, a switch valve was used to direct the exiting stream toward a Gilson fraction collector (FC-203B) or a waste bottle. Flow Commander software allowed sequential runs of multiple reaction conditions in an automated fashion.

General Procedure for Reactions in Flow. A solution of Cbz-proline (1 mmol), dimethyl maleate (1.5 mmol), catalyst 7 (0.012 mmol), 2,6-lutidine (1.2 mmol), and biphenyl (0.1 mmol) in acetonitrile (total volume of the solution 10 mL, volumetric flask) was prepared. The resulting yellow solution was degassed by bubbling dry nitrogen for 15 min. The stock solution was kept under dry nitrogen (40 mbar) to prevent introduction of oxygen. The reactor was flushed with pure acetonitrile at a flow rate of 4.00 mL/min, the lamp was ignited, and the reactor was either heated or cooled. Upon temperature stabilization, the flow rate was readjusted to reach the

desired residence time (for example, 0.333 mL/min for 30 min residence time). In every case, 10 mL of the stock solution was pumped through the reactor, but only the middle portion was collected (2 mL) to minimize dilution effects. A sample of the reaction mixture was taken, diluted in acetonitrile, and analyzed by LC/MS. The reactor was flushed with acetonitrile, and the parameters were set for the next experiment.

Experimental Procedure for Catalyst Preparation. 9-Mesityl-2,7-dimethoxy-10-phenylacridin-10-ium Tetrafluoroborate (5). A mixture of 4-methoxyaniline (7.52 g, 61.0 mmol) and 2-bromo-5-methoxybenzoic acid (10 g, 43.3 mmol) with anhydrous K₂CO₃ (8.49 g, 61.5 mmol) and copper (0.495 g, 7.79 mmol) in anhydrous 1-pentanol (150 mL) was heated at 160 °C for 3 h. The solvent was evaporated under reduced pressure, and the residue was dissolved in hot water (800 mL) and filtered through Celite. The Celite was washed with water (250 mL), and the filtrate was acidified with concentrated HCl to pH 6. A solid precipitated, which was isolated by filtration and washed with water (2 \times 150 mL). The solid was crystallized from CHCl₃ (100 mL) to give 5-methoxy-2-((4-methoxyphenyl)amino)benzoic acid (10.8 g, 39.5 mmol, 91% yield) as a light brown solid.

A mixture of 5-methoxy-2-((4-methoxyphenyl)amino)benzoic acid (10.8 g, 39.5 mmol) and polyphosphoric acid (32.4 mL) was heated to 110 °C for 3 h. The solution was poured onto ice (1000 mL), and the precipitate was filtered and washed with water (2 \times 200 mL). The precipitate was dissolved in hot EtOH (1.5 L), filtered, and evaporated to afford 2,7-dimethoxyacridin-9(10*H*)-one (6.6 g, 25.9 mmol, 65.4% yield) as a dark green solid.

In an oven-dried 250 mL round-bottom flask were charged 2,7-dimethoxyacridin-9(10*H*)-one (5.6 g, 21.94 mmol), iodobenzene (3.75 g, 18.38 mmol), copper(I) iodide (0.350 g, 1.838 mmol), 2,2,6,6-tetramethylheptane-3,5-dione (0.677 g, 3.68 mmol), and K₂CO₃ (5.08 g, 36.8 mmol) in DMF (86 mL). The round-bottom flask was equipped with a condenser, sparged with N₂ for 20 min, and heated at 120 °C under N₂ for 48 h. The reaction mixture was cooled to room temperature, diluted with water, transferred to a separatory funnel, acidified with aqueous HCl, extracted with dichloromethane, and concentrated. The crude residue was purified by chromatography on silica gel using 20% EtOAc/hexanes to yield 2,7-dimethoxy-10-phenylacridin-9(10*H*)-one (4.2 g, 12.67 mmol, 69.0% yield) as a yellow powder.

In an oven-dried 1000 mL round-bottom flask under nitrogen were charged 2,7-dimethoxy-10-phenylacridin-9(10*H*)-one (4.2 g, 12.67 mmol) and THF (420 mL, dried over 4A MS), and the reaction mixture was stirred for 30 min. A solution of mesitylmagnesium bromide (65 mL, 65.0 mmol) was added slowly at room temperature. The reaction mixture was stirred at room temperature for 24 h and at 50 °C for 24 h and then cooled to room temperature. The solution was quenched with dilute NaHCO₃ solution. This solution was extracted with DCM (3 \times 200 mL). The combined organic extracts were washed with brine, dried over Na₂SO₄, and filtered, and the solvent was evaporated under reduced pressure. The residue was purified by column chromatography on silica gel, with CH₂Cl₂/MeOH as eluent, to afford a brown solid. This solid was dissolved in Et₂O (150 mL) and stirred while a solution of tetrafluoroboric acid diethyl etherate (660 μ L, 20 mL of diethyl ether, 1.2 equiv) was added slowly. The residue was purified by preparative reverse phase HPLC (C-18), with MeOH/water + 0.1% TFA as eluent, to give 0.8 g of a yellow solid, which was stirred with a solution of tetrafluoroboric acid diethyl etherate (300 μ L, 20 mL of diethyl ether, 1.2 equiv) twice. After filtration 9-mesityl-2,7-dimethoxy-10-phenylacridin-10-ium tetrafluoroborate (0.65 g, 1.247 mmol, 9.84% yield) was obtained as a yellow solid.

¹H NMR (500 MHz, CDCl₃): δ 7.94–7.82 (*om*, 3H), 7.77 (*br s*, 2H), 7.67 (*br s*, 2H), 7.50 (*br s*, 2H), 7.18 (*s*, 2H), 6.87 (*s*, 2H), 3.78 (*s*, 6H), 2.49 (*s*, 3H), 1.90 (*br s*, 6H). ¹³C NMR (126 MHz, CDCl₃): δ 159.1, 157.5, 140.2, 137.6, 137.3, 136.2, 132.1, 131.8, 131.5, 129.8, 129.4, 128.5, 128.1, 122.2, 103.6, 56.4, 21.5, 20.5. ¹⁹F NMR (470 MHz, CDCl₃) δ -153.2. HRMS: calcd for C₃₀H₂₉BF₄NO₂⁺, 434.2115; found, 434.2140.

9-Mesityl-3,6-dimethoxy-10-phenylacridin-10-ium Tetrafluoroborate (6). In a 500 mL three-neck round-bottom flask was placed a mixture of 3-methoxyaniline (12.78 g, 104 mmol), 2-bromo-4-methoxybenzoic acid (17 g, 73.6 mmol), anhydrous K_2CO_3 (14.44 g, 104 mmol), and copper (0.842 g, 13.24 mmol) in anhydrous 1-pentanol (255 mL). The reaction mixture was heated at 160 °C for 3 h. The solvent was evaporated under reduced pressure, and the residue was dissolved in hot water (2000 mL) and filtered through Celite. The Celite was washed with water (250 mL), and the filtrate was acidified with concentrated HCl to pH 6. A solid precipitated, which was isolated by filtration and washed with water (2 × 200 mL). The solid was crystallized from $CHCl_3$ (300 mL) to give 4-methoxy-2-((3-methoxyphenyl)amino)benzoic acid (17 g, 62.2 mmol, 85% yield).

In a 250 mL three-necked round-bottom flask was placed a mixture of 4-methoxy-2-((3-methoxyphenyl)amino)benzoic acid (17 g, 62.2 mmol) and PPA (102 mL). The mixture was heated to 110 °C for 3 h. The solution was poured onto ice (2000 mL), and the precipitate was filtered and washed with water (2 × 250 mL). The precipitate was dissolved in hot EtOH (1.5 L) and filtered to afford a mixture of 1,6-dimethoxyacridin-9(10H)-one and 3,6-dimethoxyacridin-9(10H)-one (14 g, 54.8 mmol, 88% yield).

In an oven-dried 100 mL round-bottom were charged a mixture of 1,6-dimethoxyacridin-9(10H)-one and 3,6-dimethoxyacridin-9(10H)-one (14 g, 54.8 mmol), iodobenzene (9.4 g, 46.1 mmol), copper(I) iodide (0.878 g, 4.61 mmol), 2,2,6,6-tetramethylheptane-3,5-dione (1.698 g, 9.22 mmol), and K_2CO_3 (12.74 g, 92 mmol) in DMF (216 mL). The round-bottom flask was equipped with a condenser, sparged with N_2 for 20 min, and heated at 120 °C under N_2 for 48 h. The reaction mixture was cooled to room temperature, diluted with water, transferred to a separatory funnel, acidified with aqueous HCl, extracted with dichloromethane, and concentrated. The crude residue was purified by chromatography on silica gel using 20% EtOAc/hexanes to yield 14 g of product (crude, contains about 5% isomer). The crude mixture was purified by preparative Combi-Flash reverse phase HPLC (C-18), with acetonitrile/water + 0.05% NH_4HCO_3 as eluent, to give 3,6-dimethoxy-10-phenylacridin-9(10H)-one (5.8 g, 17.50 mmol, 38.0% yield) as a yellow powder.

In an oven-dried 500 mL round-bottom flask was charged 3,6-dimethoxy-10-phenylacridin-9(10H)-one (5.5 g, 16.60 mmol) in THF (275 mL) that was dried under 4A MS under nitrogen and stirred for 30 min. A solution of mesitylmagnesium bromide (55 mL, 55.0 mmol) was added slowly at room temperature. The reaction mixture was stirred at room temperature for 24 h and then at 50 °C for 24 h and cooled to room temperature, and this solution was quenched with dilute $NaHCO_3$ solution. This solution was extracted with 3 × 200 mL of DCM. The combined organic fractions were washed with brine, dried (Na_2SO_4), and filtered, and the solvent was evaporated under reduced pressure. This solid was dissolved in 150 mL of Et_2O and stirred while a solution of tetrafluoroboric acid diethyl ether complex (4.86 mL, 20 mL diethyl ether, 1.2 equiv) was added slowly. The residue was purified by preparative reverse phase HPLC (C-18), with MeOH/water + 0.1% TFA as eluent, to give 0.8 g of a yellow solid which was stirred with a solution of tetrafluoroboric acid diethyl ether complex (300 μ L, 20 mL of diethyl ether, 1.2 equiv) two times. After filtration 2.4 g of 9-mesityl-2,7-dimethoxy-10-phenylacridin-10-ium trifluoroacetate was obtained as a yellow solid, which was dissolved in 100 mL of Et_2O and stirred while a solution of tetrafluoroboric acid diethyl ether complex (1.35 mL, 20 mL diethyl ether, 1.2 equiv) was added slowly. The solid was collected by filtration to afford 9-mesityl-3,6-dimethoxy-10-phenylacridin-10-ium tetrafluoroborate (**6**; 1.45 g, 2.493 mmol, 15.02% yield) as a yellow solid.

1H NMR (600 MHz, $CDCl_3$): δ 7.96 (t, $J = 7.5$ Hz, 2H), 7.87 (t, $J = 7.7$ Hz, 1H), 7.71 (d, $J = 7.8$ Hz, 2H), 7.66 (d, $J = 9.4$ Hz, 2H), 7.24 (dd, $J = 9.5, 1.9$ Hz, 2H), 7.14 (s, 2H), 6.59 (d, $J = 1.9$ Hz, 2H), 3.83 (s, 6H), 2.47 (s, 3H), 1.87 (s, 6H). ^{13}C NMR (151 MHz, $CDCl_3$): δ 167.6, 160.7, 144.9, 140.2, 137.1, 136.2, 132.2, 132.0, 130.9, 129.5, 129.1, 128.1, 121.1, 120.3, 99.0, 56.7, 21.4, 20.2. ^{19}F NMR (470 MHz, $CDCl_3$): δ -154.2. HRMS: calcd for $C_{30}H_{29}BF_4NO_2^+$, 434.2115; found, 434.2134.

10-(3,5-Dimethoxyphenyl)-9-mesityl-1,3,6,8-tetramethoxyacridin-10-ium Tetrafluoroborate (7). Chloro[(tri-*tert*-butylphosphine)-2-(2-aminobiphenyl)]palladium(II) (0.844 g, 1.714 mmol), 1-bromo-3,5-dimethoxybenzene (49.6 g, 228 mmol), and 3,5-dimethoxyaniline (17.5 g, 114 mmol) were placed in a two-neck round-bottom flask and purged with nitrogen. Tetrahydrofuran (600 mL) was added and the solution degassed by subsurface nitrogen sparging for 15 min. A solution of sodium *tert*-butoxide (2 M, 230 mL) was added rapidly under nitrogen, and the reaction mixture was heated to 60 °C. After 19 h, the reaction mixture was cooled and 1 L of water added followed by 1.5 L of MTBE. Layers were separated and washed with MTBE and brine to obtain tris(3,5-dimethoxyphenyl)amine as a brown solid (39 g) in 81% yield.

Tris(3,5-dimethoxyphenyl)amine (41 g, 96 mmol) and 2,4,6-trimethylbenzoyl chloride (37 g, 202 mmol) were dissolved in chlorobenzene (300 mL). Triflic acid (8.51 mL, 96 mmol) was added slowly, and the mixture was heated to 80 °C. After 18 h the reaction mixture was cooled and washed with $NaBF_4$ (0.2 M, 3 × 200 mL) and water (2 × 600 mL). To the organic layer was added MTBE (2400 mL slowly) until a precipitate started to form. The mixture was seeded, and then an additional 3000 mL of MTBE was added slowly and this mixture was stirred for 30 min. The mixture was filtered, and the solid was washed with MTBE and dried under nitrogen stream, yielding a bright orange solid (44 g, 71% yield).

1H NMR (600 MHz, $CDCl_3$): δ 6.90 (s, 2H), 6.83 (t, $J = 2.1$ Hz, 1H), 6.61 (d, $J = 2.2$ Hz, 2H), 6.48 (d, $J = 2.1$ Hz, 2H), 6.18 (d, $J = 2.2$ Hz, 2H), 3.92 (s, 6H), 3.85 (s, 6H), 3.48 (s, 6H), 2.37 (s, 3H), 1.83 (s, 6H). ^{13}C NMR (151 MHz, $CDCl_3$): δ 168.4, 163.3, 162.4, 160.8, 144.9, 140.0, 137.7, 136.6, 132.2, 127.2, 113.5, 105.7, 103.0, 97.7, 92.9, 57.2, 56.7, 56.4, 21.3, 20.3. ^{19}F NMR (470 MHz, $CDCl_3$): δ -153.4. HRMS: calcd for $C_{34}H_{37}BF_4NO_6^+$, 554.2537; found, 554.2568.

9-Mesityl-1,3,6,8-tetramethoxy-10-phenylacridin-10-ium Tetrafluoroborate (8). A dried three-necked round-bottom flask was charged with 1-bromo-3,5-dimethoxybenzene (50.0 g, 230 mmol), 3,5-dimethoxyaniline (42.3 g, 276 mmol), potassium 2-methylpropanoate (83 g, 737 mmol), reactant **5** (47.7 g, 46.1 mmol), and [1,1'-biphenyl-2-yl]di-*tert*-butylphosphine (6.87 g, 23.04 mmol). The reagents were dried under reduced pressure, and the vessel was back-filled with argon. Then anhydrous toluene (750 mL) was added and the reaction mixture was heated at 80 °C for 3 h. Then iodobenzene (94 g, 461 mmol) was added and the mixture heated at 80 °C for 48 h. The mixture was cooled to room temperature and diluted with water (250 mL), and the organic layer was concentrated in vacuo. The crude product was recrystallized from MTBE/heptane in the ratio of 1/3 (2 V/6 V), affording *N*-(3,5-dimethoxyphenyl)-3,5-dimethoxy-*N*-phenylaniline (65.0 g, 164 mmol, 71.0% yield) as a gray solid.

In a 500 mL round-bottom flask were placed *N*-(3,5-dimethoxyphenyl)-3,5-dimethoxy-*N*-phenylaniline (10.00 g, 27.4 mmol) and trifluoromethanesulfonic acid (4.11 g, 27.4 mmol) in 1,4-dioxane (100 mL). To this solution was added 2,4,6-trimethylbenzoyl chloride (10.50 g, 57.5 mmol), and the mixture was stirred at 80 °C for 48 h. After rotation the crude mixture was separated by gel column chromatography (EA including 1% TFA/PE = 75/25) and 14.0 g of the crude TFA salt obtained. This was purified by reversed phase Combi-Flash HPLC (column C18-2 330 g; detector 210 nm; mobile phase A water/0.05% TFA; mobile phase B MeOH; flow rate 140 mL/min; gradient 45% B to 80% B in 20 min), and 7.40 g of the TFA salt was obtained. This TFA salt was dissolved in methanol (5 V) and the solution stirred while a solution of tetrafluoroboric acid diethyl ether complex (3.3 mL, 1.1 equiv) was added slowly. The mixture was concentrated under vacuum. After ether was added (5 V), the solid was collected after 12 h by filtration to give 9-mesityl-1,3,6,8-tetramethoxy-10-phenylacridin-10-ium tetrafluoroborate (5.70 g, 9.51 mmol, 34.8% yield) as a red-brown solid.

1H NMR (600 MHz, $CDCl_3$): δ 7.90 (t, $J = 7.7$ Hz, 2H), 7.82 (t, $J = 7.5$ Hz, 1H), 7.49 (d, $J = 7.5$ Hz, 2H), 6.91 (s, 2H), 6.48 (d, $J = 2.0$ Hz, 2H), 6.01 (d, $J = 2.1$ Hz, 2H), 3.77 (s, 6H), 3.48 (s, 6H), 2.38 (s, 3H), 1.83 (s, 6H). ^{13}C NMR (151 MHz, $CDCl_3$): δ 168.4, 162.4, 160.9, 145.3, 138.4, 137.6, 136.7, 132.3, 132.1, 131.7, 127.8, 127.2, 113.5,

97.9, 92.7, 57.2, 56.6, 21.3, 20.4. ^{19}F NMR (470 MHz, CDCl_3): δ -153.5. HRMS: calcd for $\text{C}_{32}\text{H}_{33}\text{BF}_4\text{NO}_4^+$, 494.2326; found, 494.2342.

■ ASSOCIATED CONTENT

■ Supporting Information

The Supporting Information is available free of charge on the ACS Publications website at DOI: 10.1021/acs.joc.6b01240.

^1H and ^{13}C NMR spectra and photophysical and electrochemical measurements of photocatalysts (PDF)

■ AUTHOR INFORMATION

Corresponding Author

*E-mail for D.A.D.: daniel.dirocco@merck.com.

Notes

The authors declare no competing financial interest.

■ ACKNOWLEDGMENTS

A.J.-P. is a Merck Research Laboratories Postdoctoral fellow. This research was supported by Merck Research Laboratories. A.J.-P. thanks the catalysis and automation group for their encouragement. We thank Rebecca Ruck (Merck) for helpful discussions and proofreading of this paper. Photophysical measurements were performed in the UNC-ERFC Instrumentation Facility established by the UNC-EFRC (Center for Solar Fuels, an Energy Frontier Research Center funded by the U.S. Department of Energy, Office of Science, Office of Basic Energy Sciences under Award Number DE-SC0001011).

■ REFERENCES

- (1) For reviews on the use of polypyridyl transition-metal complexes in photoredox catalysis see: (a) Prier, C. K.; Rankic, D. A.; MacMillan, D. W. C. *Chem. Rev.* **2013**, *113*, 5322. (b) Narayanam, J. M. R.; Stephenson, C. R. J. *Chem. Soc. Rev.* **2011**, *40*, 102. (c) Yoon, T. P.; Ischay, M. A.; Du, J. *Nat. Chem.* **2010**, *2*, 527. For reviews on the use of organic dyes in photoredox catalysis see: (d) Nicewicz, D. A.; Nguyen, T. M. *ACS Catal.* **2014**, *4*, 355. (e) Romero, N. A.; Nicewicz, D. A. *Chem. Rev.* **2016**, DOI: 10.1021/acs.chemrev.6b00057.
- (2) Tucker, J. W.; Stephenson, C. R. J. *J. Org. Chem.* **2012**, *77*, 1617.
- (3) Lowry, M. S.; Goldsmith, J. I.; Slinker, J. D.; Rohl, R.; Pascal, R. A., Jr.; Malliaras, G. G.; Bernhard, S. *Chem. Mater.* **2005**, *17*, 5712.
- (4) Verma, A.; Zink, D. M.; Flechon, C.; Leganes Carballo, J.; Fluegge, H.; Navarro, J. M.; Baumann, T.; Volz, D. *Appl. Phys. A: Mater. Sci. Process.* **2016**, *122*, 191.
- (5) Discekici, E. H.; Treat, N. J.; Poelma, S. O.; Mattson, K. M.; Hudson, Z. M.; Luo, Y.; Hawker, C. J.; Read de Alaniz, J. *Chem. Commun.* **2015**, *51*, 11705.
- (6) During the preparation of this paper an organic photocatalyst with redox potentials similar to those of $[\text{Ir}(\text{dF-CF}_3\text{-ppy})_2(\text{dtbpy})](\text{PF}_6)$ was reported. See: Luo, J.; Zhang, J. *ACS Catal.* **2016**, *6*, 873–877.
- (7) Nicewicz, D. A.; Nguyen, T. M. *ACS Catal.* **2014**, *4*, 355.
- (8) Fukuzumi, S.; Kotani, H.; Ohkubo, K.; Ogo, S.; Tkachenko, N. V.; Lemmetyinen, H. *J. Am. Chem. Soc.* **2004**, *126*, 1600.
- (9) (a) Hamilton, D. S.; Nicewicz, D. A. *J. Am. Chem. Soc.* **2012**, *134*, 18577. (b) Nguyen, T. M.; Nicewicz, D. A. *J. Am. Chem. Soc.* **2013**, *135*, 9588. (c) Perkowski, A. J.; Nicewicz, D. A. *J. Am. Chem. Soc.* **2013**, *135*, 10334. (d) Nguyen, T. M.; Manohar, N.; Nicewicz, D. A. *Angew. Chem., Int. Ed.* **2014**, *53*, 6198.
- (10) Romero, N. A.; Nicewicz, D. A. *J. Am. Chem. Soc.* **2014**, *136*, 17024.
- (11) Chu, L.; Ohta, C.; Zuo, Z.; MacMillan, D. W. C. *J. Am. Chem. Soc.* **2014**, *136*, 10886.

(12) Both tetrasubstituted acridiniums can be prepared in a single step from the corresponding triarylamine derivative. See the Experimental Section.

(13) For seminal work on continuous flow chemistry, see: (a) Hook, B. D. A.; Dohle, W.; Hirst, P. R.; Pickworth, M.; Berry, M. B.; Booker-Milburn, K. I. *J. Org. Chem.* **2005**, *70*, 7558. For a recent review on the topic, see: (b) Cambié, D.; Bottecchia, C.; Straathof, N. J. W.; Hessel, V.; Noël, T. *Chem. Rev.* **2016**, DOI: 10.1021/acs.chemrev.5b00707. (c) Knowles, J. P.; Elliott, L. D.; Booker-Milburn, K. I. *Beilstein J. Org. Chem.* **2012**, *8*, 2025. For a recent study comparing batch and flow photochemistry, see: (d) Elliott, L. D.; Knowles, J. P.; Koovits, P. J.; Maskill, K. G.; Ralph, M. J.; Lejeune, G.; Edwards, L. J.; Robinson, R. I.; Clemens, I. R.; Cox, B.; Pascoe, D. D.; Koch, G.; Eberle, M.; Berry, M. B.; Booker-Milburn, K. I. *Chem. - Eur. J.* **2014**, *20*, 15226.

(14) Catalyst degradation at 60 °C was much more rapid than that at room temperature.